Supporting Information

Prestoring lithium into MOF-derived MnO coated 3D carbon fiber cloth for composite lithium anode with high areal capacity and current density

Ye Liu [a], Xingtong Guo [a], Yanyan Zhou [a], Mengting Wang [a], Cheng Sun [a], Shoudong Xu [b], Xiangyun Qiu [c], Qing Huang [d], Tao Wei [a,*]

[a] *School of Energy and Power, Jiangsu University of Science and Technology, Zhenjiang 212003, China*

[b] *College of Chemical Engineering and Technology, Taiyuan University of Technology, 030024, Taiyuan, Shanxi Province, China.*

[c] *Power & Energy Storage System Research Center, College of Mechanical and Electrical Engineering, Qingdao University, Qingdao, 266071, China.*

[d] *College of Materials Science and Engineering, Nanjing Forestry University, Nanjing, 210037, China.*

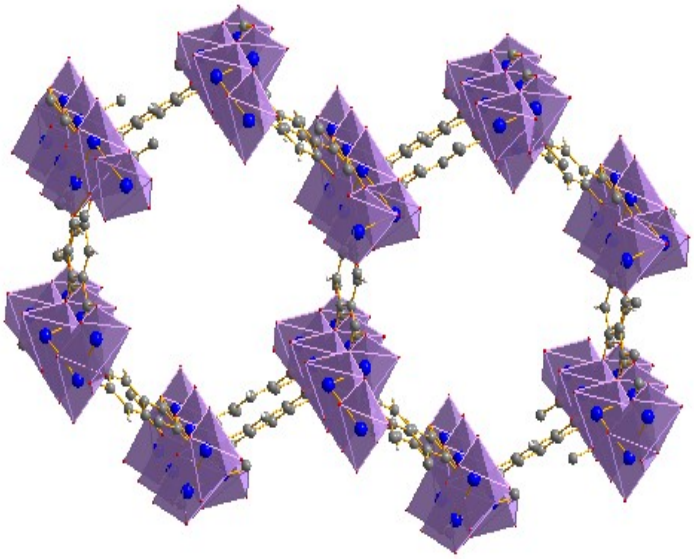

Fig S1. The structure diagram of Mn-MOF

* Corresponding author: T. Wei (wt863@126.com; wt863@just.edu.cn).

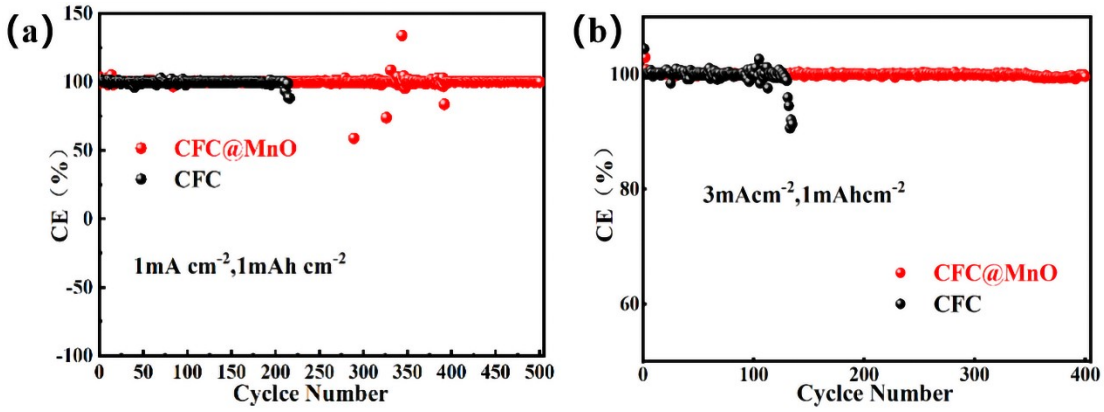

Fig S2. (a) Coulombic efficiency of CFC and CFC@MnO electrodes in half-cells at a current density of 1 mA cm-2 and a capacity density of 1 mAh cm-2. (b) Coulombic efficiency of CFC and CFC@MnO electrodes in half-cells at a current density of 3 mA cm-2 and a capacity density of 1 mAh cm-2.

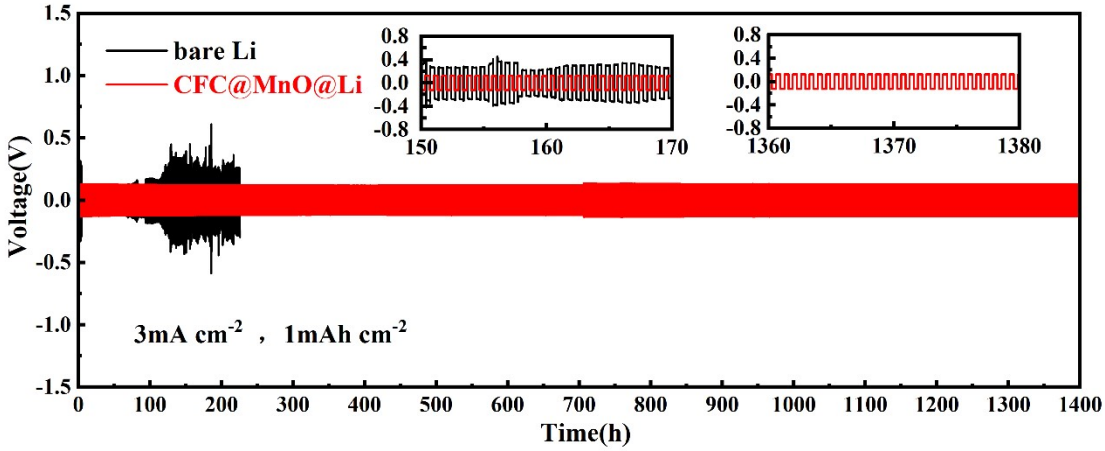

Fig S3. illustrates the cycling stability in two symmetric cells (bare Li and CFC@MnO@Li). (a) Cycling stability at a current density of 3 mA cm-2 and a cyclic capacity of 1 mAh cm-2.

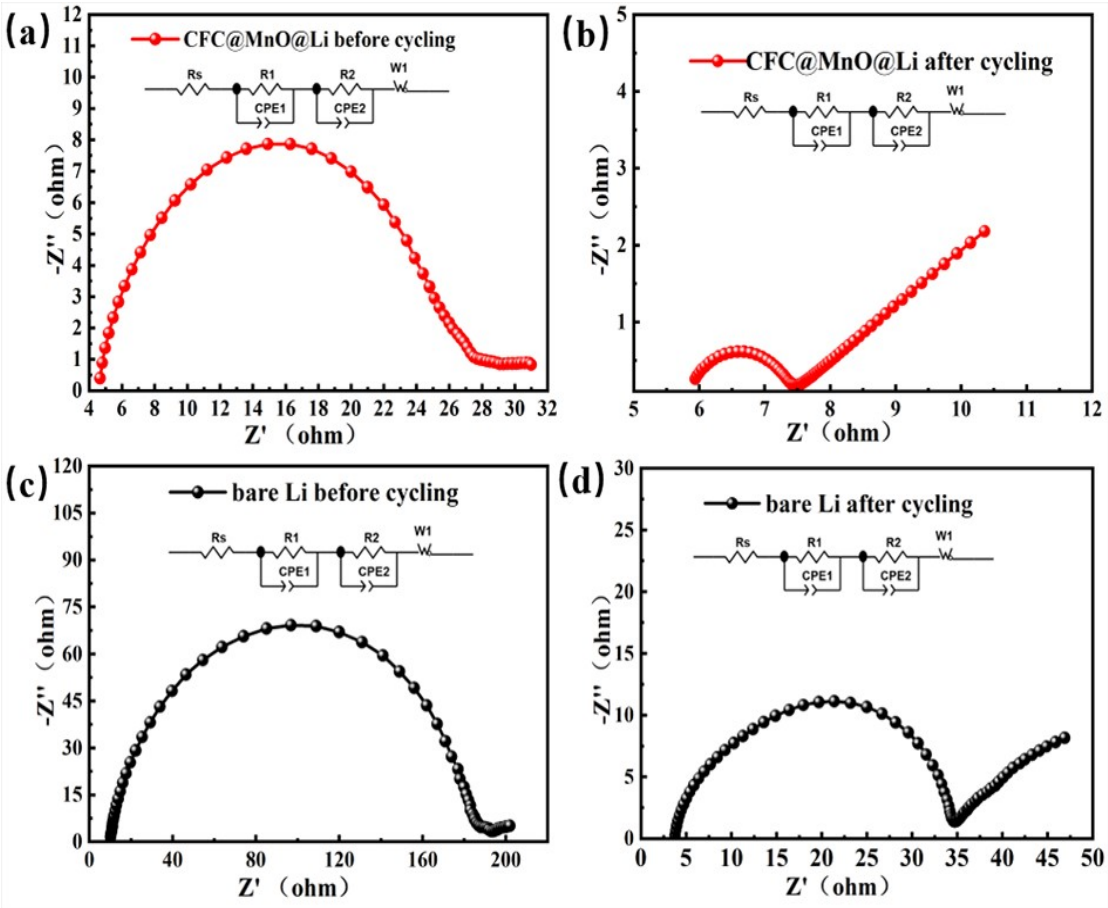

Fig S4. Nyquist plots of symmetric Li cells with different electrodes (inset shows the equivalent circuit). CFC@MnO@Li: (a) before cycling and (b) after cycling. Bare Li: (c) before cycling and (d) after cycling.

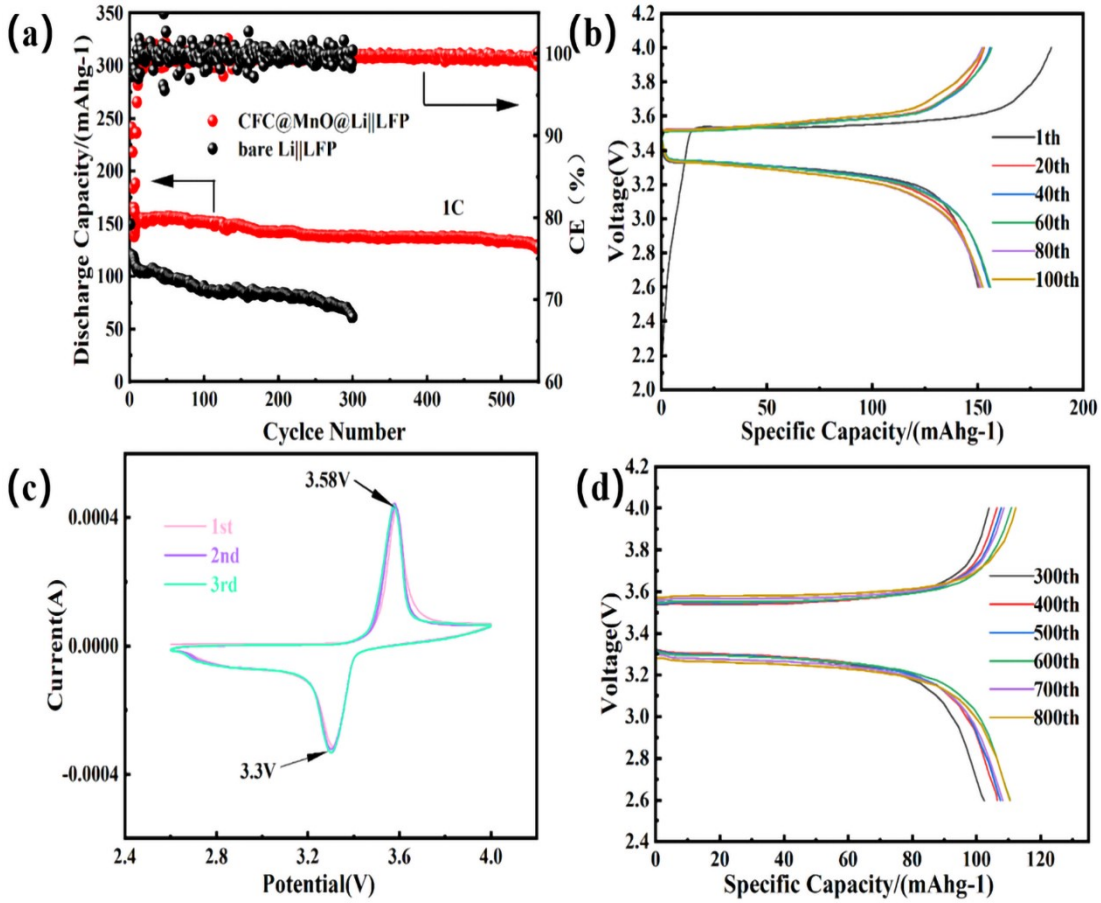

Fig S5. (a) Cycling performance of CFC@MnO@Li||LFP and bare Li||LFP cells at 1 C. (b) Cycling performance of CFC@MnO@Li||LFP cell at 1 C, represented by the corresponding charge-discharge profiles. (c) Cyclic voltammetry curves at a scan rate of 0.2 mV/s. (d) Cycling performance of CFC@MnO@Li||LFP cell at 5 C, represented by the corresponding charge-discharge profiles.

Table S1. Weight of bare Li ,CFC, CFC@MnO and CFC@MnO@Li electrode.

Materials	Average weight/ mg
CFC	22.0
CFC@MnO	25.0
CFC@MnO@Li	60.0
Li in CFC@MnO@Li electrode	35.0

Table S2. Comparison of the electrochemical performance of CFC@MnO@Li with the previous literature results.

Materials	Current density (mA cm^{-2})	Cyclic lifespan (h)	Refer.
CFC@MnO@Li	1	2300	**This work**
	3	1400	
	5	2400	
Li coated SNF skeletons	3	600	[S1]
	5	600	
Li@ZnO@CC	1	560	[S2]
	2	160	
	3	107	
CF@Sn@Li	1	1000	[S3]
	3	700	
Li-Co_3O_4-NF	1	1000	[S4]
	3	480	
3DHF-Li	1	900	[S5]
	3	320	
MCuF@Li	1	600	[S6]
	3	300	
CC@CN-Co	2	800	[S7]
	2	500	
	5	1000	

Table S3. Simulation results of equivalent circuit in Fig. S3.

	R_s/Ω	R_{int}/Ω
Bare Li (before)	5.4	160
Bare Li (after)	3.6	34.5
CFC@MnO@Li (before)	3.6	25
CFC@MnO@Li (after)	5.8	2.24

Notes: Semicircles at high and low-frequency regions in the Nyquist plots are associated with the SEI formation on the electrode surface, and the charge transfer process between the electrode/electrolyte interface, respectively. Rs: electrolyte resistance; Rf: surface film resistance; Rct: charge transfer resistance; CPE: constant phase element; W1: Warburg element (open). Rint= Rf + Rct, representing interfacial resistance between the electrode and the electrolyte.

References

[S1] Y. Xia, Y. Jiang, Y.Y. Qi, W.Q. Zhang, Y. Wang, S.F. Wang, Y.M. Liu, W.W. Sun, X.-Z. Zhao, 3D stable hosts with controllable lithiophilic architectures for high-rate and high-capacity lithium metal anodes, J. Power Sources 442 (2019) 227214.

[S2] D.Q. Jin, K. Hu, R. Hou, H. Shang, X.Y. Wang, Y. Ding, Y. Yan, H.J. Lin, K. Rui, J.X. Zhu, Vertical nanoarrays with lithiophilic sites suppress the growth of lithium dendrites for ultrastable lithium metal batteries, Chem. Eng. J. 405 (2021) 126808.

[S3] T.C. Liu, X.D. Chen, C.C. Zhan, X.H. Cao, Y.W. Wang, J.H. Liu, Selective Lithium Deposition on 3D Porous Heterogeneous Lithiophilic Skeleton for Ultrastable Lithium Metal Anodes, ChemNanoMat 6 (8) (2020) 1200-1207.

[S4] T. Wei, J.H. Lu, P. Zhang, G. Yang, C. Sun, Y.Y. Zhou, Q.C. Zhuang, Y.F. Tang, Metal-organic framework-derived Co_3O_4 modified nickel foam-based dendrite-free anode for robust lithium metal batteries, Chin. Chem. Lett. 26 (2022) 107947.

[S5] Y.Y. Qi, L. Lin, Z.L. Jian, K.Y. Qin, Y.X. Tan, Y.J. Zou, W. Chen, F.J. Li, Three-Dimensional Hierarchical Framework Loaded with Lithiophilic Nanorod Arrays for High-Performance Lithium-Metal Anodes, ChemElectroChem 7 (20) (2020) 4201-4207.

[S6] Y. Zhou, K. Zhao, Y. Han, Z.H. Sun, H.T. Zhang, L.Q. Xu, Y.F. Ma, Y.S. Chen, A nitrogen-doped-carbon/ZnO modified Cu foam current collector for high-performance Li metal batteries, J. Mater. Chem. A 7 (10) (2019) 5712-5718.

[S7] T. Zhou, J.D. Shen, Z.S. Wang, J. Liu, R.Z. Hu, L.Z. Ouyang, Y.Z. Feng, H. Liu, Y. Yu, M. Zhu, Regulating Lithium Nucleation and Deposition via MOF-Derived Co@C-Modified Carbon Cloth for Stable Li Metal Anode, Adv. Funct. Mater. 30 (14) (2020) 1909159.